Inorganic Chemistry

Article

pubs.acs.org/IC

Hydrothermal Chemistry, Structures, and Luminescence Studies of Alkali Hafnium Fluorides

Christopher C. Underwood, Colin D. McMillen, Hongyu Chen, Jeffery N. Anker, and Joseph W. Kolis*

Department of Chemistry and Center for Optical Materials Science and Engineering Technologies (COMSET), Clemson University, Clemson, South Carolina 29634-0973, United States

Supporting Information

ABSTRACT: This paper describes the hydrothermal chemistry of alkali hafnium fluorides, including the synthesis and structural characterization of five new alkali hafnium fluorides. Two ternary alkali hafnium fluorides are described: Li_2HfF_6 in space group $P\bar{3}1m$ with a = 4.9748(7) Å and c = 4.6449(9) Å and $Na_5Hf_2F_{13}$ in space group $C2/m$ with a = 11.627(2) Å, b = 5.5159(11) Å, and c = 8.4317(17) Å. Three new alkali hafnium oxyfluorides are also described: two fluoroelpasolites, K_3HfOF_5 and $(NH_4)_3HfOF_5$, in space group $Fm\bar{3}m$ with a = 8.9766(10) and 9.4144(11) Å, respectively, and $K_2Hf_3OF_{12}$ in space group $R\bar{3}m$ with a = 7.6486(11) Å and c = 28.802(6) Å. Infrared (IR) spectra were obtained for the title solids to confirm the structure solutions. Comparison of these materials was made based on their structures and synthesis conditions. The formation of these species in hydrothermal fluids appears to be dependent upon both the concentration of the alkali fluoride mineralizer solution and the reaction temperature. Both X-ray and visible fluorescence studies were conducted on compounds synthesized in this study and showed that fluorescence was affected by a variety of factors, such as alkali metal size, the presence/absence of oxygen in the compound, and the coordination environment of Hf^{4+}.

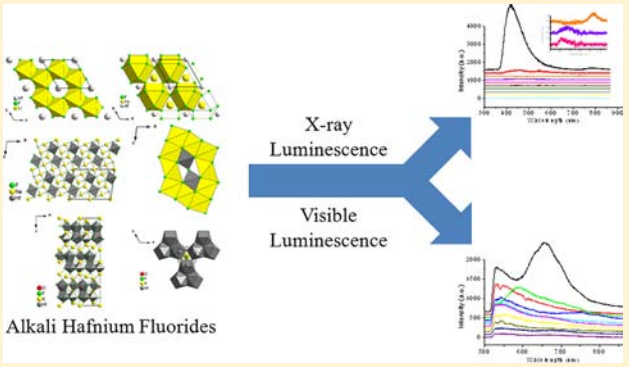

1. INTRODUCTION

Compared to other group 4 elements, the fundamental inorganic chemistry of hafnium is somewhat underexplored. Hafnium was not discovered until the 1920s,[1] and the descriptive chemistry of solid-state hafnium compounds has not received as much attention as its homologues. Since the discovery that the neutron-capture cross section of hafnium is 600 times that of its sister element zirconium,[2] its use has grown as an effective control rod in nuclear reactors (including molten fluoride-based reactors) even though the isolation of hafnium from zircon is quite expensive. Limited previous work was done primarily in molten alkali fluoride salts and led to a variety of alkali metal hafnium fluorides. Several ternary $A_xHf_yF_z$ compounds were characterized, mostly by either powder or single crystal diffraction,[3−15] with a majority of these phases being potassium hafnium fluorides. Most of the single-crystal structural characterization has centered on the A_2HfF_6 phases (A = K, Rb, Cs). Given the renewed interest in nuclear reactor safety, we feel that the fundamental descriptive chemistry of hafnium fluorides is worthy of investigation.

By way of comparison, we recently found that an extensive series of alkali thorium fluorides can be grown in hydrothermal fluids.[16−18] We previously found that the chemistry of the thorium fluorides is both extensive and interesting, and a number of long-standing issues with the compounds were clarified by the isolation of a number of unusual compounds as high-quality single crystals. Given this interesting behavior of the alkali thorium fluorides in hydrothermal fluids and the continued technological interest in hafnium chemistry, we undertook a new study of hafnium fluorides in hydrothermal fluids to compare the chemistry of the two tetravalent metal fluorides. We found that the reaction of HfF_4 with alkali fluorides in hydrothermal fluids does lead to a wide variety of new alkali metal hafnium fluoride compounds. Systematic exploration of the phase space reveals a number of compounds that reflect the size and stoichiometry of the alkali ion, as we also observed with thorium fluorides.[16−18] In contrast to the thorium fluoride system, in which we never observed any hydrolysis in hydrothermal fluids even above 600 °C, we do observe some hydrolytic reactions with hafnium fluorides to form several oxyfluorides.

In this paper, we report on our efforts to explore the alkali hafnium fluoride phase space in hydrothermal fluids. We describe the chemistry and structures of a series of new alkali hafnium fluorides and oxyfluorides grown from hydrothermal solutions, including the first ternary sodium and lithium hafnium fluorides to be characterized by single-crystal X-ray diffraction. Since earlier work with a variety of alkali zirconium oxyfluoride powders showed that they exhibit interesting X-ray

Received: August 10, 2012
Published: December 17, 2012

   dx.doi.org/10.1021/ic301760a | *Inorg. Chem.* 2013, 52, 237−244

Table 1. Specific Reaction Conditions for the Syntheses of Some Alkali Hafnium Fluorides

condition	temp (°C)	mineralizer	alkali/Hf ratio	pressure (kbar)	time (days)	crystal shape(s)	compound
1	575	4 M LiF	4.1:1	1.2	6	plates	Li_2HfF_6 ($P\bar{3}1m$) (**1**)
2	400	4 M LiF	4.1:1	0.10	5	plates	**1**
3	400	9 M LiF	9.2:1	0.10	3	plates	**1**
4	400	4 M NaF	4.1:1	0.10	6	plates, polyhedra	$Na_5Hf_2F_{13}$ ($C2/m$) (**2**), Na_3HfF_7 ($Fm\bar{3}m$)
5	400	9 M NaF	9.2:1	0.10	3	plates, polyhedra	**2**, Na_3HfF_7 ($Fm\bar{3}m$)
6	400	1 M KHF_2	1:1	0.10	5	polyhedra	$K_2Hf_3OF_{12}$ ($R\bar{3}m$) (**3**)
7	400	2 M KHF_2	2:1	0.10	4	square rods	K_2HfF_6 ($C2/c$)
8	400	9 M KHF_2	9.2:1	0.10	1	square rods, polyhedra	K_2HfF_6 ($C2/c$), K_3HfF_7 ($Fm\bar{3}m$)
9	575	1 M KF	1:1	1.2	5	needles	K_2HfF_6 ($Cmcm$)
10	575	6 M KF	6.1:1	1.2	7	polyhedra	K_3HfF_7 ($Fm\bar{3}m$)
11	575	9 M KF	9.2:1	1.2	1	polyhedra	K_3HfF_7 ($Fm\bar{3}m$)
12	400	1 M KF	1:1	0.10	3	polyhedra	K_3HfOF_5 ($Fm\bar{3}m$) (**4**)
13	400	6 M KF	6.1:1	0.10	6	polyhedra	**4**
14	400	9 M KF	9.2:1	0.10	3	polyhedra	**4**
15	400	1 M RbF	1:1	0.10	3	hex. rods, polyhedra	$Rb_5Hf_4F_{21}\cdot 3H_2O$ ($C2/c$), Rb_2HfF_6 ($P\bar{3}m1$)
16	400	2 M RbF	2:1	0.10	7	polyhedra	Rb_2HfF_6 ($P\bar{3}m1$)
17	575	2 M CsF	2:1	1.2	4	hex. rods, plates	Cs_2HfF_6 ($P\bar{3}m1$)
18	575	6 M CsF	6.1:1	1.2	5	hex. rods	Cs_2HfF_6 ($P\bar{3}m1$)
19	400	6 M CsF	6.1:1	0.10	5	hex. rods, plates	Cs_2HfF_6 ($P\bar{3}m1$)
20	400	1 M NH_4F	1:1	0.10	3	polyhedra	$(NH_4)_3HfOF_5$ ($Fm\bar{3}m$) (**5**)
21	575	1 M NH_4F	1:1	1.2	4	polyhedra	**5**
22	575	6 M NH_4F	6.1:1	1.2	5	polyhedra	**5**
23	400	6 M NH_4F	6.1:1	0.10	4	polyhedra	**5**
24	400	9 M NH_4F	9.2:1	0.10	3	polyhedra	**5**

Table 2. Crystallographic Data for Structures 1−5

	1	2	3	4	5
chemical formula	Li_2HfF_6	$Na_5Hf_2F_{13}$	$K_2Hf_3OF_{12}$	K_3HfOF_5	$(NH_4)_3HfOF_5$
fw (g/mol)	306.37	718.93	857.67	1626.92	1325.84
space group	$P\bar{3}1m$	$C2/m$	$R\bar{3}m$	$Fm\bar{3}m$	$Fm\bar{3}m$
temp/K	293 ± 2	293 ± 2	293 ± 2	293 ± 2	293 ± 2
cryst syst	trigonal	monoclinic	trigonal	cubic	cubic
a, Å	4.9748(7)	11.627(2)	7.6486(11)	8.9766(10)	9.4144(11)
b, Å		5.5159(11)			
c, Å	4.6449(9)	8.4317(17)	28.802(6)		
β, deg		97.46(3)			
V, Å^3	99.55(3)	536.19(19)	1459.2(4)	723.33(14)	834.41(17)
Z	1	2	6	1	1
D_{cal}, Mg/m^3	5.110	4.453	5.856	3.735	2.639
indices					
min	[−5, −6, −5]	[−14, −6, −10]	[−9, −9, −35]	[−9, −10, −11]	[−11, −11, −11]
max	[6, 5, 5]	[14, 6, 10]	[9, 9, 35]	[10, 10, 10]	[11, 11, 11]
params	12	55	41	8	8
F(000)	132	632	2220	728	584
μ, mm^{-1}	26.231	19.713	32.956	16.170	12.535
2θ range, deg	4.39−26.30	2.44−26.33	3.16−26.32	3.93−26.04	3.75−26.12
collected reflns	935	2418	4618	1616	1929
unique reflns	89	597	414	56	66
final R (obs data)[a]	0.0319	0.0181	0.0269	0.0290	0.0259
wR_2	0.0770	0.0449	0.0694	0.0833	0.0619
final R (all data)	0.0319	0.0184	0.0271	0.0290	0.0259
wR_2	0.0770	0.0451	0.0695	0.0833	0.0619
GOF (S)	1.215	1.164	1.294	1.386	1.291
extinction coeff	0.23(6)	0.0210(9)	0.00046(5)	0.0026(11)	0.058(12)
largest diff peak	3.008	1.233	3.137	1.500	0.997
largest diff hole	−2.662	−1.447	−2.926	−0.986	−0.522

[a] $R_1 = [\sum||F_o| - |F_c||]/\sum|F_o|$; $wR_2 = \{[\sum w[(F_o)^2 - (F_c)^2]^2]\}^{1/2}$.

dx.doi.org/10.1021/ic301760a | Inorg. Chem. 2013, 52, 237−244

Table 3. Selected Bond Distances (Å) with esd's for Compounds 1−5

Li_2HfF_6 (1) bond distances (Å)		$Na_5Hf_2F_{13}$ (2) bond distances (Å)		$K_2Hf_3OF_{12}$ (3) bond distances (Å)	
Hf1—F1 (x6)	2.017 (9)	Hf1—F1 (×2)	2.059 (3)	Hf1—F1 (×2)	2.187 (4)
Li1—F1 (x6)	2.022 (6)	Hf1—F2 (×2)	2.045 (3)	Hf1—F2 (×2)	2.133 (3)
		Hf1—F3 (×2)	2.031 (3)	Hf1—F3 (×2)	2.1321 (14)
		Hf1—F4	2.1070 (6)	Hf1—F4	1.975 (7)
		Na1—F1 (×2)	2.410 (4)	Hf1—O1	2.053 (2)
		Na1—F2 (×2)	2.394 (4)	K1—F1 (×3)	2.788 (7)
		Na1—F2 (×2)	2.440 (4)	K1—F4 (×3)	2.679 (7)
		Na1—F3 (×2)	2.516 (4)	K2—F3 (×6)	3.057 (6)
		Na2—F2 (×4)	2.302 (3)	K2—F4 (×6)	2.698 (7)
		Na2—F3 (×4)	2.600 (3)	K3—F1 (×6)	3.079 (7)
		Na3—F1 (×2)	2.301 (4)	K3—F2 (×6)	2.678 (6)
		Na3—F1 (×2)	2.389 (4)		
		Na3—F3 (×2)	2.301 (4)		

K_3HfOF_5 (4) bond distances (Å)		$(NH_4)_3HfOF_5$ (5) bond distances (Å)	
Hf1—F1 (×5)	1.953 (19)	Hf1—F1 (×5)	1.957 (14)
Hf1—O1	1.953 (19)	Hf1—O1	1.957 (14)
K1—F1 (×5)	2.535 (19)	N1—F1 (×5)	2.750 (19)
K1—O1	2.535 (19)	N1—O1	2.750 (19)
K2—F1 (×10)	3.1870 (18)	N2—F1 (×10)	3.352 (18)
K2—O1 (×2)	3.1870 (18)	N2—O1 (×2)	3.352 (18)

luminescent properties,[19] we also measured the X-ray and visible luminescent properties of the new compounds.

2. EXPERIMENTAL METHODS

2.1. Synthesis. All reagents were of analytical grade and used as purchased. Compounds in this study were prepared hydrothermally as follows: 0.10 g of HfF_4 (Aldrich, 99.9%) was combined with 0.3 mL of aqueous solutions of LiF (Aldrich, 99%), NaF (Acros, 99.9%), KF (Alfa Aesar, 99.9%), KHF_2 (Alfa Aesar, 99%), RbF (Aldrich, 99.8%), or CsF (Alfa Aesar, 99.9%), placed into a silver ampule, and weld-sealed. The concentration of the fluoride mineralizer was varied systematically over the range given in Table 1. The sealed ampule was loaded into a Tuttle-seal autoclave, which was counter pressured with additional water. The autoclave was heated at 400−600 °C for several days, typically generating a counter pressure of 2−15 kpsi, resulting in a slight compression of the welded ampules. When the reaction was complete, the contents of the ampule were filtered and the products were washed with deionized water to yield colorless crystals. Powder X-ray diffraction was used to characterize the reaction products, and single-crystal X-ray diffraction was used to identify and structurally characterize new species.

2.2. X-ray Diffraction. Powder X-ray diffraction (PXRD) data were collected using a Rigaku Ultima IV X-ray diffractometer with Cu Kα radiation (λ = 1.5418 Å). Patterns were collected from 5 to 60° in 2Θ at a scan speed of 1.0 deg/min. Single-crystal X-ray intensity data were collected using a Mercury CCD detector and a Rigaku AFC-8S diffractometer equipped with a graphite monochromator that emits Mo Kα radiation (λ = 0.71073 Å). The space groups were determined from the observed systematic absences and confirmed using the MISSYM algorithm within the PLATON program suite.[20]

Data reduction, including the application of Lorentz and polarization effects (Lp) and absorption corrections, were performed using the CrystalClear program.[21] The structures were solved by direct methods and refined using subsequent Fourier difference techniques, by full-matrix least-squares, on F^2 using SHELXTL 6.10.[22] All atoms were refined anisotropically except where specified. Data from the single-crystal structure refinements are given in Table 2. Selected bond distances are listed in Table 3. All single-crystal solutions were confirmed by simulating the powder pattern from the single-crystal structure determinations and comparing these to the powder patterns obtained from the bulk reaction products or those previously published.

2.3. IR Spectroscopy. Samples of the synthesized compounds were pressed into pellets using a KBr matrix. The spectra were collected using a Nicolet Magna-IR 550 spectrometer in a N_2-purged sample chamber, and the data were processed using the OMNIC software suite. The infrared analysis of the compounds in this study is included as the Supporting Information (text and Figures S1−S3).[38,39]

2.4. Additional Characterization. Both X-ray fluorescence and visible fluorescence were conducted on the title compounds. The X-ray luminescent spectra and fluorescent spectra were performed on a DMI5000 epifluorescent microscope (Leica Microsystems, Bannockburn, IL), equipped with a xenon light source and a DeltaNu DNS300 spectrometer. To acquire X-ray excited optical luminescent spectra, the samples were irradiated by an X-ray beam from an Amptek Mini X-ray tube (Ag target) set at 40 kV and 99 μA, and a 3 s acquisition was used. Fluorescence spectra were acquired using a Xe light source with a 460−495 nm short-pass excitation filter and 515 nm emission filter with an acquisition time of 0.1 s.

3. RESULTS AND DISCUSSION

3.1. Descriptive Synthetic Chemistry. Reactions were investigated by differing temperature, reaction time, and ratios of A/Hf (A = Li−Cs, NH_4) as a means to explore this phase space and identify any trends in compound formation. Phase-pure yields were quite common and were obtained as outlined in Table 1. It is interesting to note that the most common formulation of alkali hafnium fluorides encountered in this study is A_2HfF_6. For reactions involving lithium, this was the only phase obtained. However, this phase was not obtained for A = Na under any of our conditions, and a greater variety of chemistry is observed, producing crystals of $Na_5Hf_2F_{13}$ and Na_3HfF_7 (conditions 4 and 5). Ratios of Na/Hf below 4:1 (not included in Table 1) under similar reaction conditions repeatedly produced powders matching a powder pattern for Na_3HfF_7[12], accompanied by NaF crystals. Curiously, the formulation Na_2HfF_6 has not been observed by any other investigation. The formula A_2HfF_6 is not isostructural across

dx.doi.org/10.1021/ic301760a | Inorg. Chem. 2013, 52, 237−244

the various alkali ions. Furthermore, the structure of Li_2HfF_6 is different from that of K_2HfF_6, which is different from the Rb and Cs analogues (vida infra), so perhaps it is not surprising that there is not an apparent stable lattice for the Na analogue.

A number of potassium hafnium fluorides resulted from reactions that are varied over a range of stoichiometries and temperatures (conditions 6−14) in Table 1. In these cases, the products especially tend to be sensitive toward the acidity of the mineralizer, the reaction temperature, and the K/Hf ratio in the reaction. This sensitivity is reflected in the chemical formulas of the products and is not entirely surprising since the mineralizer serves as both the solvent and the sole source of the alkali metal ions. When an acidic mineralizer (such as KHF_2) is used, the oxyfluoride compound $K_2Hf_3OF_{12}$ (**3**) is synthesized, but it only forms from the lowest mineralizer concentrations (K/Hf < 1:1). Potassium-richer phases, such as K_2HfF_6 and K_3HfF_7, were synthesized as phase-pure products from K/Hf ratios of 2:1 to 9:1, and K/Hf > 9:1, respectively. In contrast, mineralizing with KF (conditions 9−14) leads to a different set of compounds with a sensitivity toward reaction temperature. At 400 °C (conditions 12−14), the oxyfluoride elpasolite phase K_3HfOF_5 (**4**) is the one that forms regardless of the K/Hf ratio. When the same reactions are performed at 575 °C (conditions 9−11), anhydrous K_2HfF_6 forms from K/Hf < 1:1 and K_3HfF_7 forms at K/Hf ratios above 6:1.

The formation of rubidium hafnium fluorides seems to be largely affected by adjusting the concentration of the mineralizer (conditions 15 and 16). Rb/Hf ratios smaller than 1:1 indicate favorable formation of the hydrated phase $Rb_5Hf_4F_{21}\cdot 3H_2O$, whereas Rb/Hf ratios of 1:1 and larger are favorable for the formation of trigonal Rb_2HfF_6. Much like the potassium−hafnium system, the relative ratio of Rb/Hf in the reaction is reflected in the final products in this system as well. The cesium and ammonium hafnium fluoride systems did not exhibit such a variety and appear unaffected by changes in reaction temperature or mineralizer concentrations. Regardless of the reaction conditions, only Cs_2HfF_6 and $(NH_4)_3HfOF_5$ have been observed in our study.

3.2. Crystal Structure of Li_2HfF_6 (1). Among the alkali hafnium fluorides having the A_2HfF_6 formulation synthesized during this study, we emphasize the structure of Li_2HfF_6 (**1**) since this work represents, to our knowledge, the first single-crystal structure determination of a ternary lithium hafnium fluoride. Like the isostructural zirconium fluoride,[23] the structure of **1** was determined in space group $P\bar{3}1m$ (No. 162) as opposed to $P\bar{3}m1$ (No. 164) in which the A_2HfF_6 structures based on Rb and Cs crystallize, or any of the several space groups (including $P\bar{3}m1$) adopted by the polymorphs of K_2HfF_6.[10] All atoms are located on special positions, with Hf1 having $\bar{3}1m$ symmetry, Li1 having 312 symmetry, and F1 having m symmetry.

The structure consists of the hexagonal closest packing of F^- with Li^+ and Hf^{4+} occupying octahedral holes between every other layer in a 2:1 ratio, which forms a three-dimensional layered framework of $[LiF_6]^{5-}$ and $[HfF_6]^{2-}$ octahedra. Only small angular departures from an ideal octahedron are present, with F−Li−F angles ranging from 87.8(7) to 91.2(4)° and F−Hf−F angles ranging from 89.3(5) to 90.7(5)°. The lithium fluoride octahedra propagate by edge-sharing and form sheets perpendicular to the c axis. The sheets contain hexagonal gaps with which isolated $[HfF_6]^{2-}$ octahedra are aligned (Figure 1a) in another layer. These isolated hafnium atoms are located in a separate layer sandwiched between lithium fluoride sheets

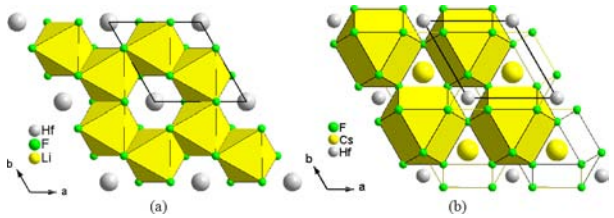

Figure 1. Structure of Li_2HfF_6 (a) as compared to Cs_2HfF_6 (b) viewed along [001], with some Cs polyhedra removed for clarity. Li atoms form $[LiF_6]^{5-}$ polyhedra, whereas Cs atoms form $[CsF_{12}]^{11-}$ polyhedra.

(Figure 2a). The two layers are connected by corner-sharing of fluorine atoms. There is only a small difference in the unit cell

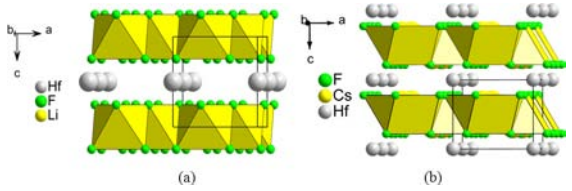

Figure 2. Layers of hafnium atoms sandwiched between $[LiF_6]^{5-}$ polyhedra in Li_2HfF_6 (a) and $[CsF_{12}]^{11-}$ polyhedra in Cs_2HfF_6 (b) viewed off [010].

parameters of **1** (vol = 99.37 (3) Å^3) compared to the zirconium analogue (vol = 99.77 Å^3), with a 0.4% contraction along the c axis differentiating the lithium hafnium fluoride.

As previously reported by Bode and Teufer,[4] the heavier alkali hafnium and alkali zirconium fluorides based on Rb and Cs have a different structure type than their lithium counterparts, crystallizing in space group $P\bar{3}m1$. We have confirmed these structure determinations using our own crystals and report this data as the Supporting Information (Table S1) as we have obtained improved R_1 values of 0.0368 (Rb_2HfF_6) and 0.0421 (Cs_2HfF_6) compared to their reports (R_1 = 0.102 for both Rb_2HfF_6 and Cs_2HfF_6). Although it is not surprising that the Rb and Cs structures have a different layer arrangement than **1** (considering both have a mixed AF_3 (A = Cs, Rb) layer packing, stacking in the cubic closest fashion with one-sixth of the Hf^{4+} occupying the octahedral holes to form sheets of $[AF_{12}]^{11-}$ polyhedra in a layered structure with isolated $[HfF_6]^{2-}$ octahedra; see Figure 1), it is interesting to note that the trend of lattice contraction for Li_2HfF_6 relative to Li_2ZrF_6 is mirrored in Rb_2HfF_6 and Cs_2HfF_6 relative to their zirconium analogues. In those systems, the unit cell volumes of the hafnium analogues are contracted by 0.6% relative to the zirconium compounds.

3.3. Crystal Structure of $Na_5Hf_2F_{13}$ (2). Compound **2** crystallizes in the monoclinic space group $C2/m$ (No. 12). Powder X-ray data simulated from our structure determination match a previously reported powder pattern for which no space group was determined. The material for the original powder pattern was assigned a nominal formulation of $2HfF_4\cdot 5NaF$ based on the melt composition from which it was prepared.[15] The structure of **2** is also isostructural to a formulation of $Na_5Zr_2F_{13}$ that was found to crystallize in the same space group.[24] However, we believe this to be the first single-crystal structure determination performed on a ternary sodium hafnium fluoride (the structure of Na_3HfF_7 was previously derived from X-ray powder films).[12] The crystallographically

dx.doi.org/10.1021/ic301760a | Inorg. Chem. 2013, 52, 237−244

unique hafnium atom forms a seven-coordinate slightly distorted square face monocapped trigonal prism with average Hf−F distances of 2.054(3) for Hf1, which correlates well with the expected value predicted by Shannon.[25] The occurrence of seven-coordinate hafnium atoms tends to be limited to pentagonal bipyramidal geometries in other alkali hafnium fluorides.[6,8] This phase contains Hf1, Na1, Na2, Na3, and F4 atoms in special positions. Hf1, Na1, and Na3 have *m* symmetry, and both Na2 and F4 have 2/*m* symmetry.

In compound **2**, pairs of seven-coordinate hafnium atoms are arranged where their caps face each other, and they corner share F4 to form a $[Hf_2F_{13}]^{5-}$ arrangement (see Figure 3).

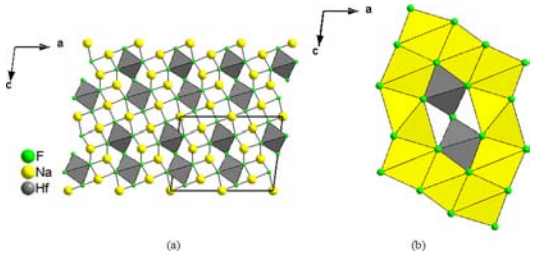

Figure 3. (a) Structure of $Na_5Hf_2F_{13}$ viewed along [010]. (b) Space-filling polyhedral view of an isolated $[Hf_2F_{13}]^{5-}$ unit surrounded by a channel of sodium fluoride polyhedra.

Bonds to the bridging atom F4 are slightly elongated (2.1070(6) Å), compared to the average of the other Hf−F bonds, which bridge to Na atoms (2.045(3) Å). The pairs of Hf−F polyhedra are both edge- and corner-sharing with Na−F polyhedra, which form a channel containing the Hf−F polyhedra. This channel is different from those of the recently reported alkali thorium fluorides[16−18] in that the tetravalent Hf, rather than the alkali metal, is contained by the channel. It may be that the smaller radius of Na (and its similar radius to Th) compared to Rb and Cs in the thorium fluorides lends itself more toward formation of the framework. The channel is shaped like an elongated hexagon when viewed along the *b* axis (Figure 3b), measuring 7.48(9) Å in length and 3.05(2) Å in diameter. Thus, the $[Hf_2F_{13}]^{5-}$ units are a rather snug fit in the channel. A three-dimensional framework of Na−F bonding fills out the remainder of the space in the structure and serves to connect the $[Hf_2F_{13}]^{5-}$ units. There are three unique sodium atoms: Na1 and Na2 are distorted square prisms, while Na3 is in a six-coordinate trigonal prismatic coordination. Edges of the distorted square prisms range from 2.542(16) to 3.02(3) Å in length for Na1, and from 2.55(4) to 3.05(2) Å in length for Na2. Comparison to the analogous zirconium structure[24,26] indicates slightly longer unit cell axes and a larger cell volume for **2**, which is to be expected considering the small difference in atomic diameter between zirconium (1.80 Å) and hafnium (1.84 Å), as described by Shannon.[25]

3.4. Crystal Structure of $K_2Hf_3OF_{12}$ (3). Compound **3** crystallizes in the trigonal space group $R\bar{3}m$ (No. 166). It is also isostructural to $Rb_2Zr_3OF_{12}$ and $Rb_2Hf_3OF_{12}$ previously found to grow from fluxes of RbF and HfF_4 in an atmosphere of Ar/HF,[5] as well as $Tl_2Zr_3OF_{12}$ grown from a melt of TlF, ZrF_4, and ZrO_2[27] and $K_2Zr_3OF_{12}$ grown by microwave-assisted hydrothermal synthesis from ZrF_4 and KOH.[28] The crystallographically unique sites consist of eight-coordinate hafnium atoms as $[HfOF_7]^{5-}$ units conforming to a distorted square antiprism geometry, with average Hf−F distances of 2.126(7) Å and a Hf−O distance of 2.053(2) Å for Hf1. All the crystallographically unique atoms are in special positions. Hf1, F2, F3, and F4 have a mirror plane on the *c* axis, K1 and O1 have 3*m* symmetry, K2 and K3 have $\bar{3}m$ symmetry, and F1 has 2-fold rotational symmetry about the *c* axis.

Three $[HfOF_7]^{5-}$ polyhedra share F4−O1 edges to form $[Hf_3OF_{18}]$ clusters. All three polyhedra in the cluster share the central O1 atom, and thus the observed Hf−O bond distance is slightly shorter (2.053(2) Å) than one may expect due to this geometrical restriction. The triangular central oxygen atom is just slightly out of plane with the hafnium atoms, allowing Hf−O−Hf angles to be slightly distorted at 115.6(2)°. Clusters propagate by corner-sharing of F3 atoms to form hafnium oxyfluoride layers in the *ab* plane. A second series of hafnium oxyfluoride clusters is joined to this first series along the *c* axis in a staggered fashion by edge-sharing pairs of F1 atoms, making the hafnium oxyfluoride layer two polyhedra thick along [001] (see Figure 4). The staggered arrangement creates

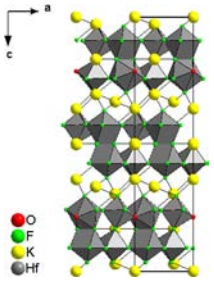

Figure 4. Layered structure of $K_2Hf_3OF_{12}$ viewed along [010].

gaps within these layers that are occupied by 12-coordinate K3 atoms. This arrangement of clusters is shown in Figure 5. Here,

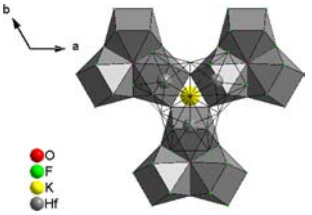

Figure 5. Staggered arrangement of $[Hf_3OF_{18}]$ clusters with gaps accommodating K3 atoms in $K_2Hf_3OF_{12}$.

K3 exhibits six longer (3.079(7) Å) and six shorter (2.678(6) Å) bonds to F1 and F2, respectively. The K3 atoms in these gaps are not completely enclosed by hafnium oxyfluoride polyhedra, as K3 is face-sharing with K1 atoms above and below the hafnium oxyfluoride layer through the long bonds to F1 atoms.

Sandwiched between the hafnium oxyfluoride layers are K1 and K2 atoms. These potassium atoms form their own layer (see Figure 4), which propagates by corner-sharing of F4 atoms. Atoms F1, F3, and F4 connect K1 and K2 to hafnium atoms by corner-sharing of F1 and F4 for K1 and by two F3 and one F4 atoms in face-sharing fashion for K2. Thus, atom F4 is centered about a planar triangle, making connections to laterally propagate the K1/K2 layer, while also connecting this layer to the hafnium oxyfluoride layer. At 1.975(7) Å, the Hf1−F4 bond is slightly shorter than usual, but similar in length to the connecting bonds in $Rb_2Zr_3OF_{12}$ and $Rb_2Hf_3OF_{12}$. In general, the hafnium oxyfluoride network appears to be quite rigid as there is very little difference between Hf−O and Hf−F

dx.doi.org/10.1021/ic301760a | *Inorg. Chem.* 2013, 52, 237−244

bonding in **3** and the analogous $Rb_2Hf_3OF_{12}$. As a result, there is only about a 1% shortening of the alkali−fluoride bond distances at the K3 site in **3** compared to the analogous Rb site in $Rb_2Hf_3OF_{12}$ since this site is confined within the hafnium oxyfluoride layers. The K1 and K2 sites, however, exhibit a 4% shortening of the alkali−fluoride bond distances compared to the analogous Rb sites, as these serve primarily as spacers for the hafnium oxyfluoride layers. This also accounts for the uneven contraction of the unit cell, where the *a* and *b* axes are contracted by 0.6% (7.648(1) vs 7.692(1) Å), whereas the *c* axis (being more influenced by the spacing between hafnium oxyfluoride layers) is contracted by about 3.5% (28.802(6) vs 29.861(6) Å) for **3** compared to $Rb_2Hf_3OF_{12}$.

3.5. Crystal Structures of K_3HfOF_5 (4) and $(NH_4)_3HfOF_5$ (5). Another interesting class of oxyfluoride crystals is those crystallizing in the cubic elpasolite structure (space group $Fm\bar{3}m$). Titanium- and zirconium-based compounds of this type have been previously explored,[29−31] but, to our knowledge, no structures of any hafnium-based oxyfluoride elpasolites have been reported. The elpasolite structure, based on the mineral K_2NaAlF_6, is a versatile structure type that commonly supports a variety of chemical substitution at the alkali metal and aluminum sites, and fluoroelpasolites are known to crystallize from hydrothermal solutions.[32,33] In the present study of new hafnium-containing elpasolites, we first used EDX to distinguish the composition of our crystals from those of the disordered fluoride K_3HfF_7, having a related structure with two fluorine atoms partially occupying 96j sites.[8] Elemental analysis always indicated the presence of oxygen at 6.5−9.1 at. % and fluorine present at 51.0−53.6 at. %, supporting a composition of A_3HfOF_5 rather than A_3HfF_7. It should be noted that attempts to solve the structures as A_3HfF_7 resulted in R_1 values as low as 0.0103, but consecutive refinements do not converge. In light of this, the structures were treated as oxyfluoride elpasolites.

A number of different crystallographic models have been determined for the titanium and zirconium oxyfluorides and peroxyfluorides of this structure type, where substitution of a tetravalent ion at the trivalent site in elpasolite requires oxygen substitution for fluorine to maintain charge balance. The first model is a simple substitutional disorder where the fluorine site (Wyckoff 24e) is $^5/_6$ occupied by fluorine and $^1/_6$ occupied by oxygen.[31,34] Models involving more complex orientational disorder (having partially occupied fluorine atoms at 24e and 96j sites with substitutional oxygen disorder at one or both of those sites) have also been used to describe the structures of $(NH_4)_3TiOF_5$ and Rb_2KTiOF_5.[29,30] These models sometimes also involve disorder and partial occupancy at the alkali metal site. In another disordered structure type, the oxygen atom is assigned $^1/_{12}$ occupancy at a 96k or 96j site, different from any of the fluorine sites in the structure. This occupancy and arrangement corresponds to a peroxy group with an O−O separation of 1.5−1.7 Å, resulting in a formula of $K_3Ti(O_2)F_5$, for example.[35−37] These related peroxyfluoro-elpasolites are also distinguishable by slightly larger unit cell parameters than the similar oxyfluoro-elpasolites.

We observe the potassium and ammonium ions in **4** and **5** to be fully ordered at 4b and 8c Wyckoff sites, having $m\bar{3}m$ and $\bar{4}3m$ site symmetries, respectively. The fluorine atom is present at the 24e site. When the substitutional model ($^5/_6$ F and $^1/_6$ O at the 24e site) was used, the R_1 values were 0.0289 and 0.0259 for the potassium and ammonium analogues, respectively. Any residual electron density appears concentrated at a 48i position 1.56 Å away from the 24e position. While a scheme of $^1/_{12}$ O occupancy at 48i and $^5/_6$ F occupancy at 24e satisfies charge balance and lowers the R_1 values (0.0197 and 0.0176 for K_3HfOF_5 and $(NH_4)_3HfOF_5$, respectively), it results in seven-coordinate K1 and eleven-coordinate K2 atoms in addition to the close O−F contact. Thus, the model of $^5/_6$ fluorine and $^1/_6$ oxygen occupancy at the 24e site appears to make the most chemical sense for the data collected and corresponding elemental analysis. The structures could be refined where potassium or ammonium ions were subject to partial occupancy at lower symmetry sites (as described by Udovenko and co-workers[29,30]), but the resulting R_1 values were slightly higher than when atoms were assigned full occupancy in the higher symmetry sites. We also attempted to disorder the fluorine and oxygen occupancies between the 24e site and a 96j site (also described by Udovenko and co-workers[29,30]), but these refinements were unsuccessful. The resulting elpasolite structures feature six-coordinate hafnium atoms having identical bond distances (within the esd) for both the potassium and the ammonium analogues. The monovalent cations are both six- and twelve-coordinate.

3.6. X-ray Luminescence Studies. X-ray luminescence studies were also conducted for the alkali hafnium fluorides synthesized in this study. Previous studies showed that hydrated alkali zirconium fluorides and oxyfluorides exhibited strong X-ray luminescence due to the excitation of their luminescent centers to excited states F* and O*.[19] Figure 6 shows the X-ray luminescence of a number of compounds prepared in this study. Broad luminescence maxima were typically observed. The hafnium-based systems seem to differ significantly from the zirconium-based systems in that the hafnium oxyfluoride, $K_2Hf_3OF_{12}$, exhibits significantly higher luminescence intensity (maximum at 410 nm) than any of the pure fluoride compounds. Interestingly, in the zirconium system, intense luminescence was observed for $Rb_2Zr_3OF_{12}$ (at 330 nm), but not $K_2Zr_3OF_{12}$. Luminescence maxima could still be identified in the comparatively weak luminescence data for $Rb_5Hf_4F_{21}\cdot 3H_2O$ (460 nm), Li_2HfF_6 (740 nm), Rb_2HfF_6 (470 nm), and Cs_2HfF_6 (410 nm). We do note that the X-ray source in this study (Ag) is different from that used by Godneva and co-workers (Mo).

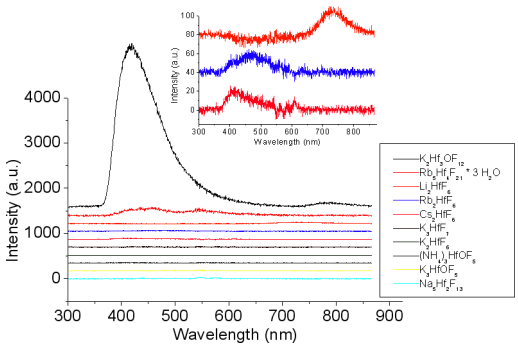

Figure 6. X-ray luminescence of the title compounds. The compounds are listed in the order of intensity (most to least) from top to bottom. The spectra were displaced vertically to facilitate their comparison.

As postulated in the previous work,[19] the structural complexity in the number of different types of bridging bonds is a likely contributor to their luminescence. This could explain why $K_2Hf_3OF_{12}$, with four types of bridging oxide and fluoride bonds creating a continuous hafnium oxyfluoride layer,

dx.doi.org/10.1021/ic301760a | *Inorg. Chem.* 2013, 52, 237−244

has a relatively strong X-ray luminescence. As a secondary contributor, the coordination number about the hafnium atoms may also play a role. We note marginally higher luminescence intensities from $Rb_5Hf_4F_{21}\cdot 3H_2O$, which contains both $[HfF_7OH_2]^{3-}$ and $[HfF_7]^{3-}$ polyhedra. Those compounds with six- coordinate hafnium (as $[HfOF_5]^{3-}$ or $[HfF_6]^{2-}$) exhibited very weak, or no luminescence. $Na_5Hf_2F_{13}$, having seven-coordinate hafnium atoms connected by a single Hf−F−Hf bridge (the $[Hf_2F_{13}]^{5-}$ unit) likewise elicited only a weak signal.

A comparison of the A_2HfF_6 compounds also gave us insight into the effects that both alkali metal size and crystallographic symmetry played in X-ray luminescence. The inset in Figure 6 displays a comparison between compounds Li_2HfF_6, Rb_2HfF_6, and Cs_2HfF_6, which shows that the luminescence maxima shift to lower energies with decreasing alkali metal size. However, Li_2HfF_6 exhibits a slightly greater luminescence intensity than its Cs and Rb counterparts. This is perhaps due to the crystallographic differences between them; Cs_2HfF_6 and Rb_2HfF_6 contain $[CsF_{12}]^{11-}$ and $[RbF_{12}]^{11-}$ polyhedra in a layered structure with $[HfF_6]^{2-}$ octahedra as compared to the layered framework of $[LiF_6]^{5-}$ and $[HfF_6]^{2-}$ octahedra in compound Li_2HfF_6. Comparing the luminescence of the three trigonal compounds to the negligible luminescence from orthorhombic K_2HfF_6 could indicate improved luminescence with higher symmetry in this particular family of compounds.

3.7. Visible Luminescence Studies. Visible luminescence studies were also conducted for the alkali hafnium fluorides synthesized in this study. Previous studies showed that hafnium compounds of the type Cs_2HfX_6 (X = Cl, Br, I) exhibit significant luminescence in the visible region,[40] whereas a related hafnium oxide, Li_2HfO_3, exhibits luminescence in the UV range.[41] Figure 7 shows the luminescence of a number of

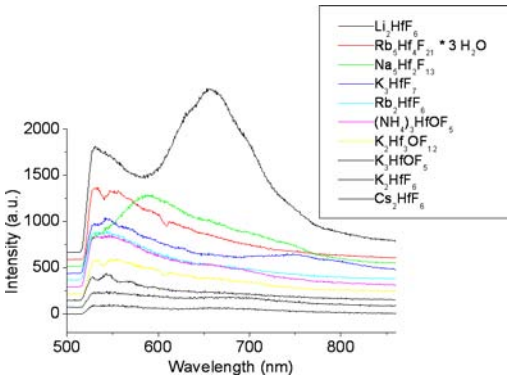

Figure 7. Visible fluorescence spectra of the title compounds. The compounds are listed in the order of intensity (most to least) from top to bottom. Emission wavelengths less than 515 nm were cut off with a long-pass emission filter. The spectra were displaced vertically to facilitate their comparison.

compounds prepared in this study using visible excitation. Similar to the X-ray luminescence, broad emission maxima were typically observed; they are based on the electronic transition of $A_{1g} \rightarrow T_{1u}$ that Ackerman observed for his luminescence measurements of alkali hafnium halides at room temperature.[40]

Comparison of the 2−1−6 structure types shows that trigonal compounds **1**, Rb_2HfF_6, and Cs_2HfF_6 exhibit both increased luminescence and maxima shifts to higher energies with the decreasing size of the alkali metal. Similar to the observations with their X-ray luminescence, compound **1** displays more luminescence than its Cs and Rb counterparts (perhaps, again, due to the same crystallographic differences described in the previous section) and the intensity of the luminescence tends to increase with decreasing alkali metal size. When comparing these three trigonal compounds to orthorhombic K_2HfF_6, it also shows that the coordination environment around Hf^{4+} must also be taken into consideration ($[HfF_6]^{2-}$ for the trigonal formulations compared with $[HfF_7]^{3-}$ for the orthorhombic formulation[10]), though it may not affect luminescence as significantly. We must note again that we have only seen this trend apply to compounds of the same formulation. Comparing oxygen-containing compounds **3**, **4**, **5**, and $Rb_5Hf_4F_{21}\cdot 3H_2O$ shows that only the hydrated compound has significantly more luminescence. The fact that $Rb_5Hf_4F_{21}\cdot 3H_2O$ also contains mixed coordination environments for Hf^{4+} ($[HfF_7]^{3-}$ and $[HfF_8]^{4-}$) may also factor into its luminescence. Though the coordination environments around the Hf^{4+} for the oxyfluorides differ (disordered $[HfOF_5]^{3-}$ for **4** and **5**, $[HfOF_7]^{5-}$ for **3**), it does not seem to affect luminescence. The unexpectedly high luminescence of **2** can also be explained by its Hf^{4+} coordination environment. Of all the alkali hafnium fluorides investigated, only **2** contains corner-sharing $[HfF_6]^{2-}$ polyhedra, which may drastically alter the luminescence of these compounds. When comparing the luminescence of all the alkali hafnium fluorides used in this study, there does not seem to be a correlation between the group symmetry of the compounds and their luminescence.

4. CONCLUSIONS

In this paper, we describe a variety of diverse chemical results all related to the alkali hafnium fluorides. All the products and chemistry we elucidate results from hydrothermal reactions. We performed the reactions over a range of stoichiometries and temperatures in an attempt to cover a broad region of phase space. New hafnium fluorides were characterized for all the alkali metals as well as for NH_4^+. A majority of products were characterized as high-quality single crystals, and these provided comparative examples to zirconium where appropriate. In some cases, the products are new structures, and in others, they were reported previously as powder samples made from melts. The single crystal determination is provided here.

We isolated a number of members of the A_2HfF_6 formulation, including Li_2HfF_6, which represents, to our knowledge, the first example of a structure of Li-containing hafnium fluoride. Interestingly, we have been unable to isolate any example of the unknown Na_2HfF_6 formula. The heavier analogues of A_2HfF_6 (A = K, Rb, Cs) were isolated in good yield and are structurally analogous to the previously reported melt reactions. We also isolated a number of more structurally complex alkali hafnium fluorides, such as $Na_5Hf_2F_{13}$ and K_3HfF_7. Although the metal fluoride structural chemistry is not as subtle and complex as we observed previously in the thorium fluoride system, the chemistry is somewhat richer in the sense that we do observe some new hydrolytic oxyfluoride products (such as $K_2Hf_3OF_{12}$, K_3HfOF_5, and $(NH_4)_3HfOF_5$) in the hafnium system as well as a hydrated species ($Rb_5Hf_4F_{21}\cdot 3H_2O$). No such oxygen-containing examples were observed by us in the thorium system. In general, we see that the alkali fluoride chemistry is more similar to that of zirconium than thorium.

Given the previous observation that alkali zirconium oxyfluorides demonstrate bright X-ray luminescence, we performed X-ray luminescence on our compounds and also

dx.doi.org/10.1021/ic301760a | Inorg. Chem. 2013, 52, 237−244

observed bright luminescence for the oxyfluoride $K_2Hf_3OF_{12}$. This is somewhat reminiscent of the observation of bright luminescence of $Rb_2Zr_3OF_{12}$, although the emission is somewhat red shifted for our material (440 nm) versus 330 nm for the zirconium material. On the basis of previous observations of visible luminescence for other alkali hafnium halides, visible luminescence studies were also conducted on our compounds, and we found that Li_2HfF_6 exhibits bright luminescence compared to the other compounds in the study. This shows that changing the alkali metal can also affect both visible luminescence intensity and maxima instead of only changing the halide.

■ ASSOCIATED CONTENT

Ⓢ Supporting Information

Listings of CIF files for **1**−**5**, crystallographic data for Cs_2HfF_6 and Rb_2HfF_6 (Table S1), and IR analysis and spectra of compounds **2**, **3**, **5**, Rb_2HfF_6, and $Rb_5Hf_4F_{21}{\cdot}3H_2O$ (Figures S1−S3). This material is available free of charge via the Internet at http://pubs.acs.org.

■ AUTHOR INFORMATION

Corresponding Author

*E-mail: kjoseph@clemson.edu.

Notes

The authors declare no competing financial interest.

■ ACKNOWLEDGMENTS

The authors thank the National Science Foundation Grant no. DMR-0907395 for financial support.

■ REFERENCES

(1) Coster, D.; von Hevesy, G. *Naturwissenschaften* **1923**, *11*, 133.
(2) Itkin, I. *Analysis of the Neutron Capture Cross Section and Resonance Integral of Hafnium*; Report no. WAPD-TM-324; U.S. Government Printing Office: Washington, D.C., 1962.
(3) Gerasimenko, A. V.; Bukvetskii, B. V.; Logvinova, V. B.; Davidovich, R. L. *Russ. J. Coord. Chem.* **1991**, *17*, 793−796.
(4) Bode, H.; Teufer, G. *Z. Anorg. Allg. Chem.* **1956**, *283*, 18−25.
(5) Koller, D.; Müller, B. G. *Z. Anorg. Allg. Chem.* **2002**, *628*, 575−579.
(6) Gusev, A. I.; Chuklanova, E. B.; Kuznetsov, V. Y.; Rogachev, D. L. *Russ. J. Inorg. Chem.* **1991**, *36*, 937−938.
(7) Chernyshov, B. N.; Didenko, N. A.; Bakeeva, N. G.; Bukvetskii, B. V.; Gerasimenko, A. V. *J. Struct. Chem.* **1991**, *36*, 1004.
(8) Granzin, J.; Saalfeld, H. *Z. Kristallogr.* **1988**, *183*, 71−76.
(9) Neumann, C.; Saalfeld, H.; Gerdau, E.; Guse, W. *Z. Kristallogr.* **1986**, *175*, 159−164.
(10) Saalfeld, H.; Guse, W. *Neues Jahrb. Mineral., Abh.* **1983**, *146*, 29−40.
(11) Neumann, C.; Granzin, J.; Saalfeld, H. *Z. Kristallogr.* **1988**, *184*, 221−227.
(12) Harris, L. *Acta Crystallogr.* **1959**, *12*, 172.
(13) Plitzko, C.; Meyer, G. *Z. Anorg. Allg. Chem.* **1998**, *624*, 169−170.
(14) Plitzko, C. Ph.D. Dissertation, Hannover University, Hannover, Germany, 1999.
(15) Thoma, R. E. *Phase Diagrams of Nuclear Reactor Materials*; Report no. ORNL-2548; U.S. Government Printing Office: Washington, D.C., 1959.
(16) Underwood, C. C.; Mann, M.; McMillen, C. D.; Kolis, J. W. *Inorg. Chem.* **2011**, *50*, 11825−11831.
(17) Underwood, C. C.; Mann, M.; McMillen, C. D.; Musgraves, J. D.; Kolis, J. W. *Solid State Sci.* **2012**, *14*, 574−579.
(18) Underwood, C.; McMillen, C.; Kolis, J. *J. Chem. Crystallogr.* **2012**, *42*, 606−610.
(19) Godneva, M. M.; Motov, D. L.; Boroznovskaya, N. N.; Klimkin, V. M. *Russ. J. Inorg. Chem.* **2007**, *52*, 661−666.
(20) Spek, A. L. *PLATON: A Multipurpose Crystallographic Tool*; Utrecht University: Utrecht, The Netherlands, 2003.
(21) *CrystalClear*; Rigaku/MSC: The Woodlands, TX, 1999.
(22) Sheldrick, G. *Acta Crystallogr., Sect. A* **2008**, *64*, 112−122.
(23) Hoppe, R.; Dähne, W. *Naturwissenschaften* **1960**, *47*, 397−397.
(24) Herak, R. M.; Malcic, S. S.; Manojlovic, L. M. *Acta Crystallogr.* **1965**, *18*, 520−522.
(25) Shannon, R. *Acta Crystallogr., Sect. A* **1976**, *32*, 751−767.
(26) Shaoya, M.; Youjun, K.; Jinxiao, M.; Manrong, L.; Zanbin, W.; Xueyan, W.; Thai, Z. J. *Jiegou Huaxue* **2006**, *25*, 173−179.
(27) Mansouri, I.; Avignant, D. *J. Solid State Chem.* **1984**, *51*, 91−99.
(28) Saada, M. A.; Hemon-Ribaud, A.; Maisonneuve, V.; Smiri, L. S.; Leblanc, M. *Acta Crystallogr., Sect. E* **2003**, *59*, i131−i133.
(29) Udovenko, A. A.; Laptash, N. M.; Maslennikova, I. G. *J. Fluorine Chem.* **2003**, *124*, 5−15.
(30) Udovenko, A. A.; Laptash, N. M. *Acta Crystallogr., Sect. B* **2011**, *67*, 447−454.
(31) Vedrine, A.; Belin, D.; Besse, J. P. *Bull. Soc. Chim. Fr.* **1972**, *1972*, 76−78.
(32) Goryunov, A. V.; Popov, A. I.; Khajdukov, N. M.; Fedorov, P. P. *Mater. Res. Bull.* **1992**, *27*, 213−220.
(33) da Fonseca, R. J. M.; Tavares, A. D., Jr.; Silva, P. S.; Abritta, T.; Khaidukov, N. M. *Solid State Commun.* **1999**, *110*, 519−524.
(34) Pausewang, G.; Rüdorff, W. *Z. Anorg. Allg. Chem.* **1969**, *364*, 69−87.
(35) Massa, W.; Pausewang, G. *Mater. Res. Bull.* **1978**, *13*, 361−368.
(36) Schmidt, R.; Pausewang, G. *Z. Anorg. Allg. Chem.* **1986**, *537*, 175−188.
(37) Schmidt, R.; Pausewang, G.; Massa, W. *Z. Anorg. Allg. Chem.* **1986**, *535*, 135−142.
(38) Antokhina, T. F.; Ignat'eva, L. N.; Kaidalova, T. A.; Savchenko, N. N. *Russ. J. Coord. Chem.* **2003**, *29*, 157−162 (supporting information).
(39) Neumayer, D. A.; Cartier, E. *J. Appl. Phys.* **2001**, *90*, 1801−1808 (supporting information).
(40) Ackerman, J. F. *Mater. Res. Bull.* **1984**, *19*, 783−791.
(41) Schipper, W. J.; Piet, J. J.; De Jager, H. J.; Blasse, G. *Mater. Res. Bull.* **1994**, *29*, 23−30.